Agulhas leakage as a key process in the modes of Quaternary climate changes

Thibaut Caley[a,1,2], **Jacques Giraudeau**[a], **Bruno Malaizé**[a], **Linda Rossignol**[a], **and Catherine Pierre**[b]

[a]University of Bordeaux, Centre National de la Recherche Scientifique, Environnements et Paléoenvironnements Océaniques et Continentaux, Unité Mixte de Recherche 5805, F-33400 Talence, France; and [b]University of Pierre et Marie Curie, Unité Mixte de Recherche 7159, Laboratory of Oceanography and Climate: Experiments and Numerical Approaches, Institut Pierre Simon Laplace, Boîte 100-4, place Jussieu, 75252 Paris Cedex 05, France

Edited by Paul G. Falkowski, Rutgers, The State University of New Jersey, New Brunswick, Brunswick, NJ, and approved March 1, 2012 (received for review September 22, 2011)

Heat and salt transfer from the Indian Ocean to the Atlantic Ocean (Agulhas leakage) has an important effect on the global thermohaline circulation and climate. The lack of long transfer record prevents elucidation of its role on climate changes throughout the Quaternary. Here, we present a 1,350-ka accumulation rate record of the planktic foraminiferal species *Globorotalia menardii*. We demonstrate that, according to previous assumptions, the presence and reseeding of this fauna in the subtropical southeast Atlantic was driven by interocean exchange south of Africa. The Agulhas transfer strengthened at glacial ice-volume maxima for every glacial-interglacial transition, with maximum reinforcements organized according to a 400-ka periodicity. The long-term dynamics of Agulhas leakage may have played a crucial role in regulating meridional overturning circulation and global climate changes during the Mid-Brunhes event and the Mid-Pleistocene transition, and could also play an important role in the near future.

Modeling results have shown that Agulhas leakage dynamics affects variability in Atlantic meridional overturning circulation (AMOC) and global climate (1–3). Paleo studies also suggest an important role of the Agulhas leakage for the climate system (4–8). Nonetheless, modulations of Agulhas leakage prior to about 550 ka are unknown. This lack of information prevents elucidation of (*i*) forcing mechanisms governing the Agulhas leakage on longer time interval, and (*ii*) the potential role of the Agulhas exchange throughout the critical period of the Mid-Pleistocene transition (MPT) which saw the settling of high-amplitude, low-frequency glacial variability (9).

Here, we present a continuous, high-resolution 1,350-ka record of accumulation rate (AR) of the tropical species *Globorotalia menardii* (see *Materials and Methods*) at Ocean Drilling Program (ODP) Site 1087 (31°28′S, 15°19′E, 1,371-m depth) located in the southern Benguela region (Fig. 1), in close vicinity to the Cape of Good Hope. A previously established age model for Site 1087 based on $\delta^{18}O$ measurements in planktic and benthic foraminifera was revised here by correlating this stable isotope record with the LR04 stack (10) (*Materials and Methods*).

Results and Discussion

***G. menardii* as a Tracer of Past Indian to Atlantic Leakage South of Africa.** Although presently thriving in the tropical and subtropical Atlantic (Fig. 1), *G. menardii* exhibits drastic and near-synchronous changes in abundances at the scale of this ocean realm throughout the Brunhes and Matuyama chronozones (11, 12). Given the continuous presence of this species in planktic foraminiferal assemblages of Indian and Pacific marine sediments throughout the Quaternary (*SI Appendix*, Fig. S1 *A* and *B*), as well as the processes of interocean exchange of surface and intermediate waters presently taking place south of Africa (13), we assume, according to previous suggestions (14–18), that abundance changes of this species in sedimentary archives of the SE Atlantic can be used as reliable tracer of past Indian to Atlantic leakage south of Africa.

ODP Site 1087 was drilled on the continental margin of SW Africa, slightly shoreward of the southeast-northwest-oriented core track of Agulhas shed rings and filaments in the SE Atlantic (13). Although this location explains the overall low contribution of tropical species to the foraminiferal assemblages at the studied site (16), a separate observation of the whole, unsplit >125-μm fraction, indicates that specimens of *G. menardii*, although rare, are near-continuously present at Site 1087 and are affected by large-amplitude abundance changes throughout the last 1,350 ka (Fig. 2*A*).

In order to confirm *G. menardii* as a tracer of interocean exchange in the SE Atlantic, we compare our record obtained at Site 1087 with a previous, approximately 550-ka-long paleorecord obtained from a nearby core and based on the relative abundance of "Agulhas leakage fauna (ALF)" (4) (Fig. 1 and Fig. 2*B*). Both records compare well (Fig. 2 and *SI Appendix*, Fig. S2) and indicate that extreme leakage events are strongly expressed by peak concentrations and accumulation rates of *G. menardii* at ODP Site 1087, whereas periods of reduced Indian to Atlantic transfer are marked by minimum, if not absence of our planktonic foraminiferal tracer species.

Given the proposed mechanism involved in the abundance changes of *G. menardii* in the SE Atlantic, one can argue that part, if not most, of the pattern recorded at ODP Site 1087 might be a function of the abundance of this taxon within its source area in the Indian Ocean. We therefore compare our proxy record off southwest Africa with a mid to late Quaternary record of concentration and AR of *G. menardii* from a coring site located in the precursor area of the Agulhas current (core MD96-2048; Figs. 1 and 2*C*) (*Materials and Methods*). From this comparison, none of the large-amplitude abundance events recorded at ODP Site 1087 has any equivalent in the Agulhas source area, hereby indicating that our tracer record in the SE Atlantic is independent of the dynamics of this taxon in the Indian Ocean. Our *G. menardii* record therefore stands as a reliable tracer of Agulhas leakage to the SE Atlantic, and provides a continuous history of interocean exchange south of Africa for the last 1,350 ka. The dynamics of Indian to Atlantic transfer at orbital scales will be discussed elsewhere (*SI Appendix*, Section 1 and Fig. S3 *A* and *B*), so here we focus on the long-term variability of Agulhas leakage associated to important paleoceanographic events.

Reseeding of *G. menardii* in the Tropical-Subtropical Atlantic. Major transfer events based on the AR of *G. menardii* at Site 1087

Author contributions: T.C., J.G., and B.M. designed research; T.C., J.G., and L.R. performed research; T.C., J.G., B.M., and C.P. analyzed data; and T.C., J.G., and B.M. wrote the paper.

The authors declare no conflict of interest.

This article is a PNAS Direct Submission.

[1]To whom correspondence should be addressed. E-mail: t.caley@vu.nl.

[2]Present address: Faculty of Earth and Life Sciences, Vrije Universiteit De Boelelaan 1085, 1081 HV, Amsterdam, The Netherlands.

This article contains supporting information online at www.pnas.org/lookup/suppl/doi:10.1073/pnas.1115545109/-/DCSupplemental.

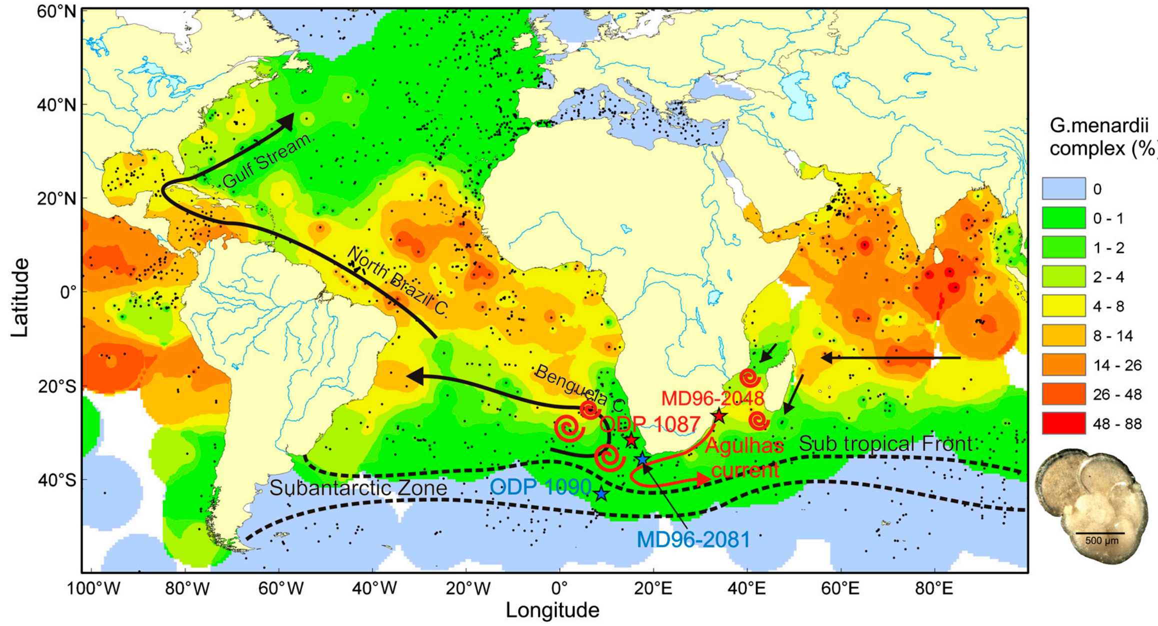

Fig. 1. Abundance (wt %) of the tropical species *Globorotalia menardii* in surface sediments of the World Ocean (compilation from the MARGO database; see *Materials and Methods*). Schematic view of the main oceanic surface circulation involved in the transfer of this taxon into the Atlantic Ocean via the Agulhas current is indicated. The studied sites (ODP 1087 and MD96-2048), reference sites (MD96-2081, ref. 4 and ODP 1090, refs. 22 and 23), and locations of the STF and the SZ are also indicated.

(Fig. 2*A*) are enlightened by the late Quaternary succession of this taxon (presence/absence) in the tropical and subtropical Atlantic (11, 12, 19, 20) (Fig. 2). AR of *G. menardii* at ODP Site 1087 show distinct important increases that are near-synchronous with the position of the S/T, U/V, W/X, and Y/Z zonal boundaries in the tropical Atlantic as well as with subzonal transitions (T4/T3, T3/T2, V3/V2, and V2/V1) (Fig. 2) (*Materials and Methods*). As long as variations in *G. menardii* AR are a function of the volume of Indian Ocean thermocline water transferred to the southeast Atlantic, our record is evidence for the role of this mechanism in the reseeding of this taxon in the tropical Atlantic over the last 1,350 ka. Although the absence of *G. menardii* in the tropical and subtropical Atlantic during certain intervals (S, U, W, and Y) stays an enigma (15), our record suggests that sustained reduced Agulhas transfer prior to these periods (Fig. 2) might be involved into this extinction process.

Long-Term Agulhas Leakage Changes: Forcing and Climatic Impact. As previously observed for the last *ca.* 550 ka (4), our *G. menardii* record indicates that each of the 17 terminations of the last 1,200 ka is affected by an increased transfer of Agulhas water to the SE Atlantic (Fig. 3 *A* and *B*). A lower frequency pattern of strengthened and sustained intensification according to a *ca.* 400-ka periodicity is strongly expressed by our proxy record (Fig. 3*B*), and displays increased amplitudes from 1,350 ka onward.

We propose that this observed pattern of interocean exchange is resulting from latitudinal migration of the subtropical front (STF) as previously suggested for shorter timescales (4, 5, 21) (northward migration of the STF south of Africa inducing reduced Agulhas leakage). In order to test this hypothesis, we compare our results with records of ice rafted detritus (an indicator for the presence of icebergs) and sea surface temperature (SST) reconstructions obtained at ODP Site 1090 (22, 23) (Fig. 3 *C* and *D*) which monitor past meridional changes in the position of both the subantarctic zone (SZ) and the STF in the Southern Ocean (Fig. 1). An overall tendency of southward migration of the STF (Fig. 3 *C* and *D*) is associated with increased amplitudes of interocean exchanges (Fig. 3*B*). Peak northward positions of the STF and SZ during glacials are organized according to a 400-ka periodicity (Fig. 3 *C* and *D*), and slightly precede strengthened Agulhas leakage events (Fig. 3*B*). A recent study (5) indicates that the extreme northward position of the STF during glacial marine isotopic stages (MIS) 12 and 10 (around 400 ka) is responsible of the reappearance and abundance in the SE Atlantic of the ALF due to the deglacial strengthening of the

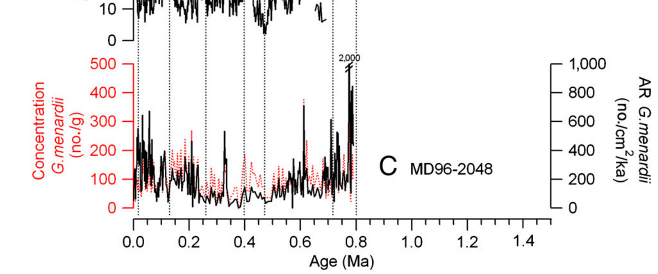

Fig. 2. Mid- to late-Quaternary reseeding of *G. menardii* in the tropical-subtropical Atlantic. (*A*) Concentration and AR of *G. menardii* at ODP Site 1087 in the southern Benguela region. (*B*) Relative abundance of Agulhas Leakage Fauna (ALF) at Cape Basin (4). Note that a new age model for core MD96-2081 was built based on the correlation between the δ^{18}O of the benthic foraminifer and the LR04 stack to allow comparison with our dataset. This new age model extends the previous record of Peeters et al. (4) from 550 to approximately 700 ka. (*C*) Concentration and AR of *G. menardii* at site MD96-2048 in the SW Indian Ocean. The top frame indicates the *G. menardii* zones in the tropical-subtropical Atlantic as defined by Ericson and Wollin (11) and according to the revised stratigraphy of Martin et al. (19, 20) (green/white frames point to the presence/absence of the taxon, respectively) (see *Materials and Methods*). Dashed lines indicate events of reseeding in the tropical-subtropical Atlantic Ocean.

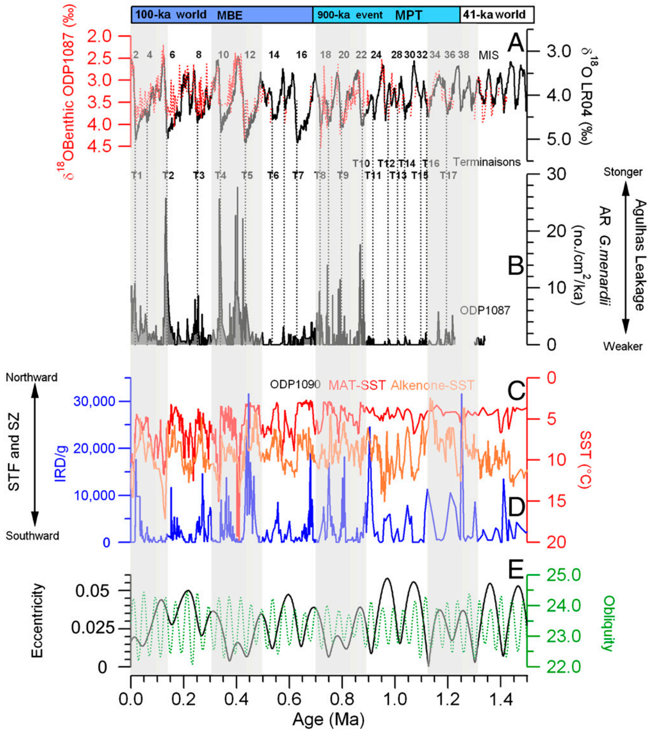

Fig. 3. Coupled histories of Agulhas leakage and STF migration over the last 1,350 ka. (*A*) δ^{18}O of benthic foraminifera *Planulina wuellerstorfi* at ODP Site 1087 and comparison with the LR04 stack (10) (see *Materials and Methods*). Glacial marine isotopic stages and terminations are indicated. (*B*) Agulhas leakage as inferred from AR of *G. menardii* at ODP Site 1087. Fine dashed lines point to reinforcement of transfer at terminations. Gray frames indicate sustained periods of transfer strengthening according to a 400-ka periodicity. (*C* and *D*) Concentrations of Ice Rafted Detritus (IRD) and SST reconstruction at ODP Site 1090 as tracers of meridional shifts in the location of the STF and SZ (22, 23). (*E*) Eccentricity and obliquity cycles over the last 1,500 ka (43). Top frame indicates the MPT (the 900-ka event and the MBE are also indicated) (9, 25).

Indian–Atlantic connection. This pattern is well documented in our record (Fig. 3*B*).

Interestingly, all the periods of successive, extreme northward positions of the STF correspond to important changes in modes of global climate variability over the Quaternary. Indeed, the periods centered at 800 ka B.P. and 1,200 ka B.P. roughly bracket the MPT (9) (Fig. 3). The MPT, starting at 1,025 ka B.P. and completed at 700 ka B.P. (9), saw the emergence of low-frequency (100-ka cycles), high-amplitude glacial variability, for so far unknown reasons (24). The period centered at 400 ka B.P. corresponds to the Mid-Brunhes event (MBE) (25) and is characterized by a further increase of ice-volume variations leading to four large-amplitude 100-ka glacial–interglacial cycles from then to present.

The important northward position of the STF every 400 ka could be a response to both cooler global climates (26) and anomalously cool equatorial temperatures (5). Indeed, a minimum of eccentricity every 400 ka might reduce the Hadley cell (27) (cool tropical SST), drawing the STF northward (Fig. 3 *D* and *E*). A reduction of obliquity amplitude occurs around 800 ka B.P. and, although of minor amplitude, at 1,200 ka B.P. (Fig. 3*E*). Caley et al. (6) have shown the importance of this parameter for controlling the Agulhas current system via its role on latitudinal migration of the STF and associated westerlies. Concerning the effect of global cooling, recent studies suggested that the climate/dust/CO_2 feedback might play an important role, in particular across the MPT (24, 28). The global coccolithophoride production varied with a *ca.* 400-ka periodicity (29) and could affect the global carbon cycle although the p_{CO2} changes during the Pleistocene could be compensated biogeochemically (29) or masked by higher frequency cycles in the record. Future modeling experiments could be helpful to better constrain forcings on the STF shifts.

The Agulhas leakage is supposed to have important effect on thermohaline circulation and ice-volume modulation (1–7). Benthic δ^{13}C gradients between the Atlantic and the Pacific Oceans, used as a ventilation proxy (5) (Fig. 4*A*), are indicative of high-amplitude changes in Atlantic overturning and/or in Pacific ventilation throughout the last 1,500 ka according to a 400-ka periodicity. This long-term variability in the strength of Atlantic overturning is phased with meridional shifts of the STF and SZ, which (*SI Appendix*, Fig. S4), as explained above, modulate the efficiency of the Indian–Atlantic transfer of thermocline waters. This observation supports the idea that the Agulhas leakage played an important role on the dynamics of the global overturning circulation over long timescales. This hypothesis is in agreement with a recent modeling study showing that a northward shift of the westerlies caused a contraction of the subtropical gyres in the southern hemisphere, which both reduced the Agulhas leakage and North Atlantic deep-water formation (30).

We argue that changes in Agulhas leakage constitute therefore a key internal process leading to the major climate shifts of the Quaternary period—i.e., the MPT and the MBE.

Strengthening of the Agulhas leakage may have induced a resumption of the AMOC during terminations and a more vigorous AMOC during the interglacial periods of the last 450 ka (Fig. 4). The resumption could have promoted more heat transport to northern high latitudes, warming of the northern hemisphere, and northward movement of the intertropical convergence zone (31). We confirm, for long time periods, that the Agulhas leakage can constitute a precursor for the reestablishment of full interglacial conditions.

Our interglacial period (the Holocene) is included into a new cycle of 400 ka (Fig. 3). Our study indicates that this configuration, together with long-term tendency in Agulhas leakage changes (Fig. 4), could be favorable for an important strengthening of Indian–Atlantic transfer, itself leading to a more stable and vigorous AMOC (3, 4, 32) (*SI Appendix*, Fig. S5). A recent work also suggests that anthropogenic forcing contributed to increased Agulhas leakage during the past decades (21), a pattern which is projected to continue and accelerate during the 21st century (33). Both the natural climate configuration enlightened by our study and the modern anthropogenic perturbation are therefore prone

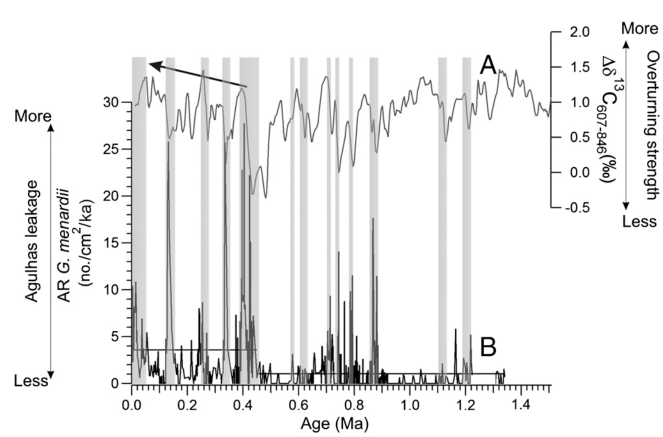

Fig. 4. Link between the Agulhas leakage and ocean overturning changes. (*A*) $\Delta\delta^{13}$C as an indicator of the overturning strength (5). (*B*) Agulhas leakage as inferred from AR of *G. menardii* at ODP Site 1087. Increased leakage during terminations is triggered by deglacial strengthening of Indian–Atlantic transfer. This process leads to an increase of overturning and a potential resumption of the AMOC (32). Long-term changes in Agulhas leakage (horizontal lines and arrow) seem to induce a more vigorous AMOC during the interglacial periods of the last 450 ka.

to an important role for the transfer of heat and salt from the Indian Ocean to the Atlantic Ocean in the near future, with important implications on the freshwater budget and the deep-water formation in the subpolar North Atlantic (2, 3).

Materials and Methods

***G. menardii* Accumulation Rate.** Because of the scarcity of *G. menardii* in planktic foraminiferal assemblages at ODP Site 1087, we conducted a separate count of this species on the total unsplit >125-μm fraction. We subsequently expressed *G. menardii* abundance as both concentration (number of specimens/g bulk sediment) and AR (number of specimens/cm^2/ka) according to the formula AR = concentration × SR × DBD, where SR (sedimentation rate in centimeters per thousand years) equals sedimentation rate after conversion of original depth (meters below seafloor) into corrected depth (meters composite depth) and construction of the final age model. Dry bulk density in grams per cubic centimeter $(\mathrm{DBD}) = 2.65 \times (\text{gamma-ray attenuation bulk density} - 1)/(2.65 - 1)$. The same method was used to calculate the AR of *G. menardii* in core MD96-2048 off Mozambique. In this study, *G. menardii* refers to the complex assemblage which combines *G. menardii* spp. and *Globorotalia tumida* without distinction of the different morphotypes or subspecies.

***G. menardii* Abundance and Multiproxy Approach for the Reconstruction of the Glacial Ocean Surface (MARGO) Database.** The modern and last glacial maximum distributions (wt %) of *G. menardii* in the World Ocean (Fig. 1 and *SI Appendix*, Fig. S1*A*) were interpolated from the MARGO database (34–36) using the ArcGIS Geographic Information System software.

Age Models. The oxygen isotope stratigraphy at ODP Site 1087 is based on δ^{18}O measurements on shell on the benthic and planktic foraminifera *Planulina wuellerstorfi* and *Globorotalia inflata*, respectively. The timescale calibration of the inferred isotopic stages was previously published for the 0- to 400-ka (37) and for 400- to 1,500-ka (38) intervals, and was revised in the present study by correlating the δ^{18}O records with the LR04 benthic stack (10) (Fig. 3) using Analyseries software (39). The age model for core MD96-2048 is taken from Caley et al. (6). All the data in Figs. 2–4 are plotted according to the LR04-based age model (10).

Age of *G. menardii* Biozones in the Tropical-Subtropical Atlantic. The ages of biozones are essentially based on Martin et al. (19, 20), which revised the Ericson and Wollin (11) zonation scheme for the Caribbean, dividing the Pleistocene interval into 17 zones and subzones with an average resolution of approximately 100 ka. Whereas the boundary ages of zones Z to T are relatively well constrained, the results are more uncertain for transition T4/S and S/R. According to Martin et al. (19, 20), the T4/S boundary is located within MIS 24–25 (*ca.* 940 ka B.P. on the LR04 age scale). A more recent study (40) confirms that the T4/S boundary seems occur after the Jaramillo, which is dating at 990 ka (41). By correlation with magnetostratigraphy and oxygen isotope stratigraphy proposed by Wei (42) this result gives an occurrence after MIS 26. For the R/S boundary, we choose the ideal zonation of Martin et al. (20) (*ca.* 1,200 ka).

ACKNOWLEDGMENTS. Marine samples for site ODP 1087 were provided by the Ocean Drilling Program (ODP), sponsored by the National Science Foundation and participating countries. Frederique Eynaud is acknowledged for the *G. menardii* photo. This is Past4Future contribution no. 16. The research leading to these results has received funding from the European Union's Seventh Framework programme (FP7/2007-2013) under Grant 243908, "Past4Future. Climate change—Learning from the past climate." Centre National de la Recherche Scientifique (CNRS) Institut National des Sciences de l'Univers Les Enveloppes Fluides et l'Environnement-Evolution et Variabilité du climat à l'Echelle globale program "MOMIES" (moussons massives et incongrues) is also acknowledged for financial support. This paper is contribution 1842 of Unité Mixte de Recherche 5805 Environnements et Paléoenvironnements Océaniques et Continentaux, University Bordeaux 1/CNRS.

1. Biastoch A, Boning CW, Lutjeharms JRE (2008) Agulhas leakage dynamics affect decadal variability in Atlantic overturning circulation. *Nature* 456:489–492.
2. Beal LM, De Ruijter WPM, Biastoch A, Zahn R, and SCOR/WCRP/IAPSO Working Group 136 (2011) On the role of the Agulhas system in ocean circulation and climate. *Nature* 472:429–436.
3. Weijer W, De Ruijter WPM, Sterl A, Drijfhout SS (2002) Response of the Atlantic overturning circulation to South Atlantic sources of buoyancy. *Glob Planet Change* 34:293–311.
4. Peeters FJC, et al. (2004) Vigorous exchange between the Indian and Atlantic oceans at the end of the past five glacial periods. *Nature* 430:661–665.
5. Bard E, Rickaby EM (2009) Migration of the subtropical front as a modulator of glacial climate. *Nature* 460:380–383.
6. Caley T, et al. (2011) High-latitude obliquity as a dominant forcing in the Agulhas current system. *Clim Past* 7:1285–1296.
7. Dickson AJ, et al. (2010) Atlantic overturning circulation and Agulhas leakage influences on southeast Atlantic upper ocean hydrography during marine isotope stage 11. *Paleoceanography* 25:PA3208.
8. Franzese AM, Hemming SR, Goldstein SL (2009) Use of strontium isotopes in detrital sediments to constrain the glacial position of the Agulhas retroflection. *Paleoceanography* 24:PA2217.
9. Clark PU, et al. (2006) The middle Pleistocene transition: Characteristics, mechanisms, and implications for long-term changes in atmospheric pCO2. *Quat Sci Rev* 25:3150–3184.
10. Lisiecki LE, Raymo ME (2005) A Pliocene-Pleistocene stack of 57 globally distributed benthic δ^{18}O records. *Paleoceanography* 20:PA1003.
11. Ericson DB, Wollin G (1968) Pleistocene climates and chronology in deep-sea sediments. *Science* 162:1227–1234.
12. Ruddiman WF (1971) Pleistocene sedimentation in the equatorial Atlantic: Stratigraphy and faunal paleoclimatology. *Geol Soc Am Bull* 82:283–302.
13. Lutjeharms JRE (2006) *The Agulhas Current* (Springer, Berlin).
14. Charles CD, Morley JJ (1988) The paleoceanographic significance of the radiolarian Didymocyrtis tetrathalamus in eastern Cape Basin sediments. *Palaeogeogr Palaeoclimatol Palaeoecol* 66:113–126.
15. Berger WH, Wefer G (1996) *The South Atlantic: Past and Present Circulation*, eds G Wefer, WH Berger, G Siedler, and DJ Webb (Springer, Berlin), pp 363–410.
16. Giraudeau J, Pierre C, Herve LA (2000) Late Quaternary high-resolution record of planktonic foraminiferal species distribution in the southern Benguela region: SITE1087. *Proc Ocean Drill Prog Sci Res* 175:1–26.
17. Rau AJ, et al. (2002) A 450-kyr record of hydrological conditions on the western Agulhas Bank Slope, south of Africa. *Mar Geol* 180:183–201.
18. Berger WH, Vincent E (1986) Sporadic shutdown of North Atlantic deep water production during the Glacial-Holocene transition? *Nature* 324:53–55.
19. Martin RE, Johnson GW, Neff ED, Krantz DE (1990) Quaternary planktonic foraminiferal assemblage zones of the Northeast gulf of Mexico, Colombia basin (Caribbean sea), and tropical Atlantic Ocean: graphic correlation of microfossil and oxygen isotopes datums. *Paleoceanography* 5:531–555.
20. Martin RE, Neff ED, Johnson GW, Krantz DE (1993) Biostratigraphic expression of Pleistocene sequence boundaries, Gulf of Mexico. *PALAIOS* 8:155–171.
21. Biastoch A, Boning CW, Schwarzkopf FU, Lutjeharms JRE (2009) Increase in Agulhas leakage due to poleward shift of Southern Hemisphere westerlies. *Nature* 462:495–498.
22. Becquey S, Gersonde R (2002) Past hydrographic and climatic changes in the Subantarctic Zone of the South Atlantic-The Pleistocene record from ODP Site 1090. *Palaeogeogr Palaeoclimatol Palaeoecol* 182:221–239.
23. Martínez-Garcia A, Rosell-Melé A, McClymont EL, Gersonde R, Haug GH (2010) Subpolar Link to the emergence of the modern equatorial Pacific cold tongue. *Science* 328:1550–1553.
24. Hönisch B, Hemming NG, Archer D, Siddall M, McManus JF (2009) Atmospheric carbon dioxide concentration across the Mid-Pleistocene transition. *Science* 324:1551–1554.
25. Jansen JHF, Kuijpers A, Troelstra SRA (1986) Mid-Brunhes climatic event: Long-term changes in global atmosphere and ocean circulation. *Science* 232:619–622.
26. Williams GP, Bryan K (2006) Ice age winds: An aquaplanet model. *J Clim* 19:1706–1715.
27. Ashkenazy Y, Gildor H (2008) Timing and significance of maximum and minimum equatorial insolation. *Paleoceanography* 23:PA1206.
28. Martínez-Garcia A, et al. (2011) Southern Ocean dust-climate coupling over the past four million years. *Nature* 476:312–315.
29. Rickaby REM, et al. (2007) Coccolith chemistry reveals secular variations in the global ocean carbon cycle? *Earth Planet Sci Lett* 253:83–95.
30. Sijp WP, England MH (2008) The effect of a northward shift in the southern hemisphere westerlies on the global ocean. *Prog Oceanogr* 79:1–19.
31. Sepulcre L, Vidal L, Tachikawa K, Rostek F, Bard E (2011) Sea-surface salinity variations in the northern Caribbean Sea across the Mid-Pleistocene Transition. *Clim Past* 7:75–90.
32. Knorr G, Lohmann G (2003) Southern Ocean origin for the resumption of Atlantic thermohaline circulation during deglaciation. *Nature* 424:532–536.
33. Sen Gupta A, et al. (2009) Projected changes to the Southern Hemisphere Ocean and sea ice in the IPCC AR4 climate models. *J Clim* 22:3047–3078.
34. Barrows TT, Steve J (2005) Sea-surface temperatures around the Australian margin and Indian Ocean during the last glacial maximum. *Quat Sci Rev* 24:1017–1047.
35. Hayes A, Kucera M, Kallel N, Sbaffi L, Rohling EJ (2005) Glacial Mediterranean sea surface temperatures based on planktonic foraminiferal assemblages. *Quat Sci Rev* 24:999–1016.
36. Kucera M, et al. (2005) Reconstruction of sea-surface temperatures from assemblages of planktonic foraminifera: Multi-technique approach based on geographically constrained calibration datasets and its application to glacial Atlantic and Pacific Oceans. *Quat Sci Rev* 24:951–998.
37. Pierre C, Saliege JF, Urrutiaguer MJ, Giraudeau J (2001) Stable isotope record of the last 500 K.Y. at site 1087 (southern cape basin). *Proc Ocean Drill Prog Sci Res* 175:1–22.
38. McClymont EL, Rosell-Mele A, Giraudeau J, Pierre C, Lloyd JM (2005) Alkenone and coccolith records of the mid-Pleistocene in the south-east Atlantic: Implications for the UK37 index and South African climate. *Quat Sci Rev* 24:1559–1572.
39. Paillard D, Labeyrie LD, Yiou P (1996) Macintosh program performs time-series analysis. *EOS Trans Am Geophys Union* 77:379.

40. Nishi H, Norris RD, Okada H (2000) Paleoceanography changes in the dynamics of subtropical Atlantic surface conditions at Hole 997A. *Proc Ocean Drill Prog Sci Res* 164:343–363.
41. Berggren WA, et al. (1995) Late Neogene chronology: New perspectives in high-resolution stratigraphy. *Geol Soc Am Bull* 107:1272–1287.
42. Wei W (1993) Calibration of upper Pliocene-lower Pleistocene nannofossil events with oxygen isotope stratigraphy. *Paleoceanography* 8:85–99.
43. Laskar J, et al. (2004) A long-term numerical solution for the insolation quantities of the Earth. *Astron Astrophys* 428:261–285.

SUPPLEMENTARY INFORMATION

The Agulhas leakage as a key process in the modes of Quaternary climate changes

Thibaut Caley, Jacques Giraudeau, Bruno Malaizé, Linda Rossignol, Catherine Pierre.

Section 1: Orbital scale Agulhas leakage at site ODP1087

Independent orbital age models are required to address the role of orbital forcing on the Quaternary dynamics of Agulhas leakage. The oxygen isotope stratigraphy of ODP Site 1087 is based on the orbitally-derived LR04 age scale (1). To solve the problem of orbital dependency, we developed another approach based on the so-called depth-derived stack H07 (2) which is not relying upon orbital assumptions (Fig. S3-A).

The *G. menardii* transfer index is ideal to investigate interocean exchanges on long time-scale but is less adapted for documenting the history of leakage at the scale of orbital changes. Indeed, gaps of data occur in the benthic stratigraphy of ODP Site 1087 (Fig. S3-A). This limitation in mind, and because the orbital forcing on Agulhas leakage has been investigated over the last 550 ka (3), we focused our interpretation on supra-orbital scale changes over the last 1,350 ka.

A B-Tukey cross correlation analysis using Analyseries software (4) (time interval 0-1,200 ka, 2 ka step) between *G. menardii* record and ETP (constructed by normalizing and stacking eccentricity, tilt and negative precession) on the LR04 and H07 age models indicates some weak differences suggesting that a small part of the variance observed with the LR04 age model is linked to its $\delta^{18}O$ tuning with orbital parameters (Fig. S3-B). However, weak spectral power signal in the precession band (23 ka cycle), and more important power in the 41 ka (obliquity) and 100 ka cycles are observed with the H07 age model. These results confirm Caley et al. (5) and Peeters et al. (3) assumptions that mid- to late Quaternary changes in the Agulhas current system are essentially driven by 41 and 100 ka cycles over the last 800 ka. The 400 ka cycle is also visible (Fig. S3-B).

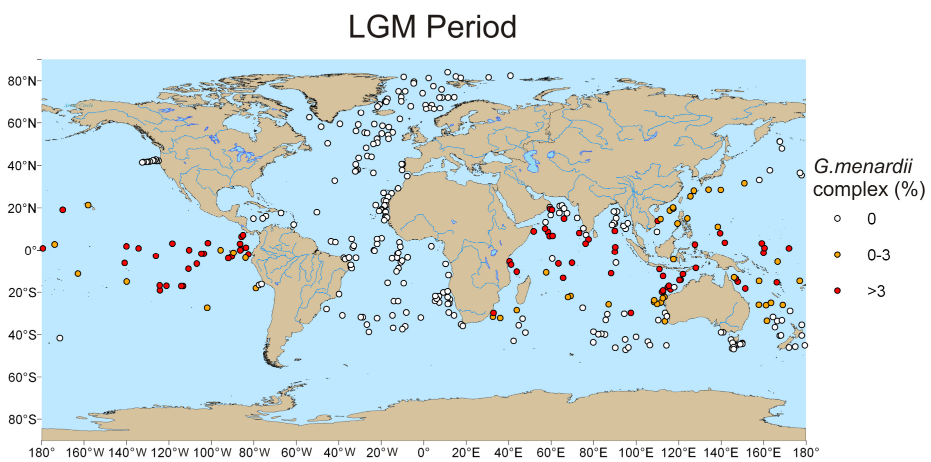

Fig. S1-A): Global distribution (wt%) of the *Globorotalia menardii* complex during the Last Glacial Maximum (LGM) (compiled from the PANGAEA-hosted MARGO database (6-8)) showing the absence (presence) of this foraminiferal taxon in the Atlantic Ocean (tropical-subtropical Indo-Pacific ocean).

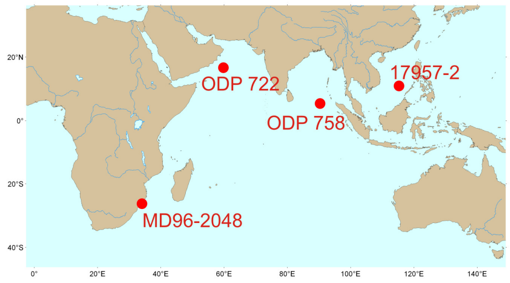

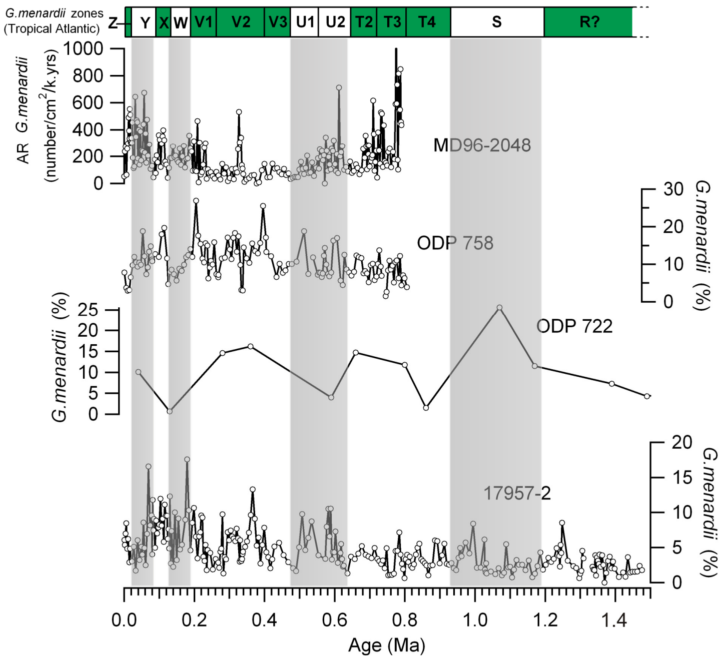

Fig. S1-B): Distribution (wt%) of *G. menardii* in Indian and Pacific sediment cores providing evidence for the continuous presence of this species complex in this tropical-subtropical ocean realm throughout the last 1,500 ka (MD96-2048: this study; ODP 722 (9); ODP 758 (10), 17957-2 (11)). The grey boxes refer to the periods where *G. menardii* is absent from the tropical-subtropical Atlantic according to the foraminiferal zonation scheme given in the top frame.

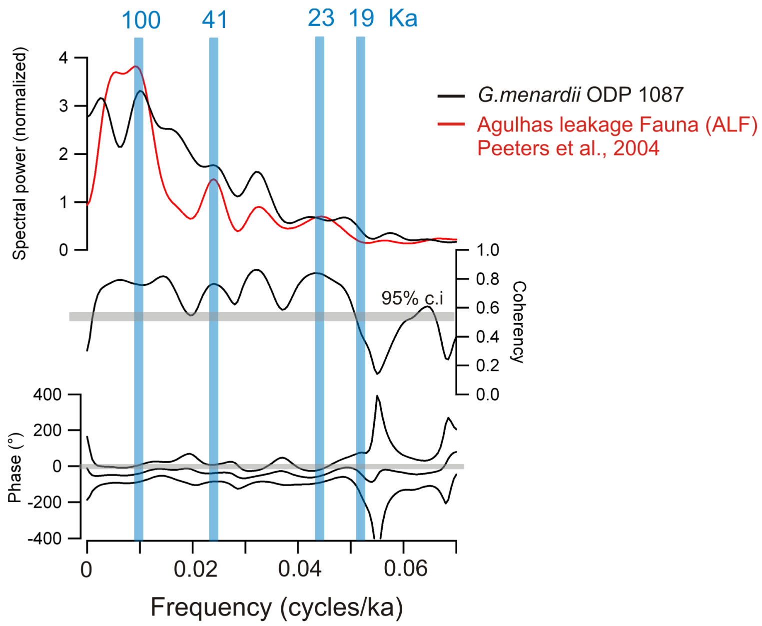

Fig. S2: Cross-correlation analysis confirming the relationship between the Agulhas leakage fauna (ALF) (3) and the ODP 1087 *G. menardii* AR records of Indian-Atlantic interocean exchange. This B-Tukey analysis (time interval 0-630 ka, 2.15 ka step) was performed using the Analyseries software (4). The horizontal grey line indicates the 95% confidence level for the coherency. We observed a high coherency in the 100, 41 and 23 ka bands with no significant phase offset between records. Both records appear therefore closely related in spectral power and phasing.

A)

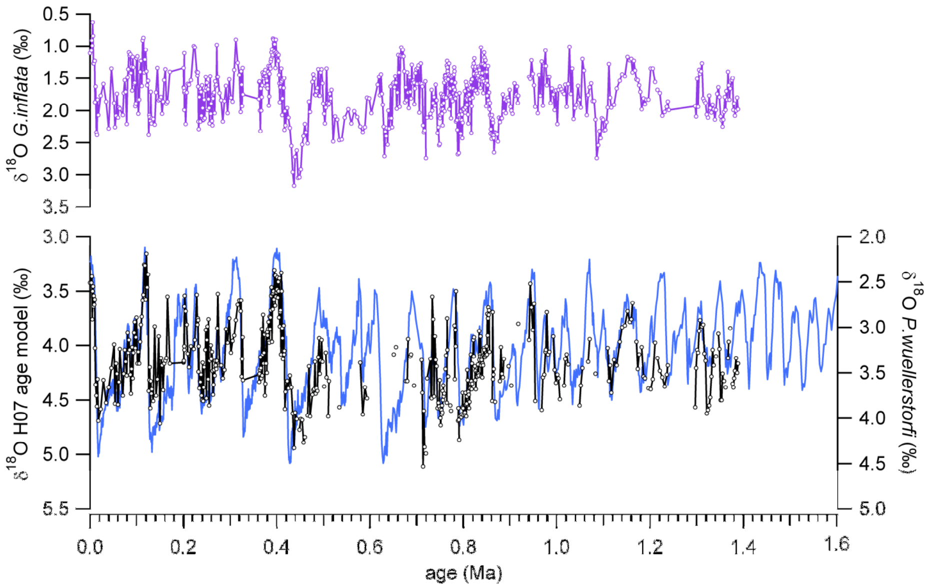

B)

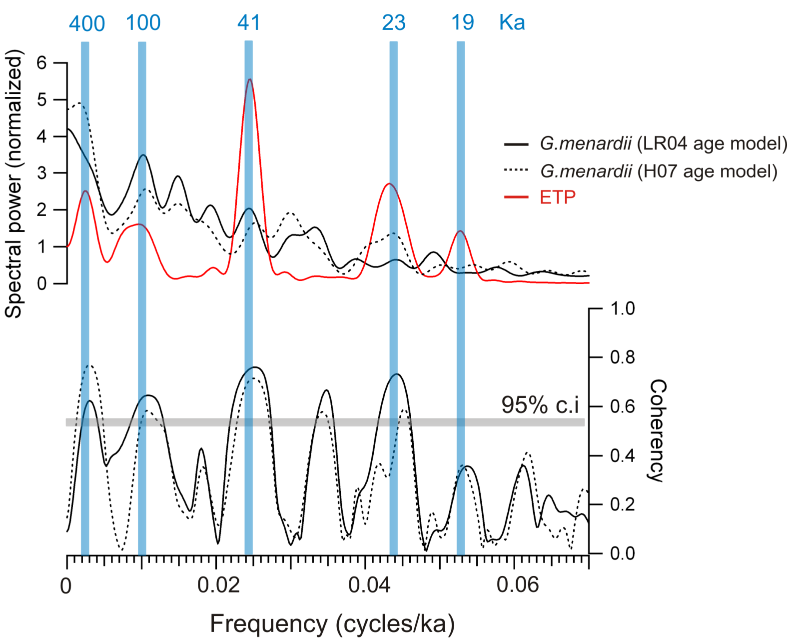

Fig. S3: Alternative stratigraphy (see section 1).

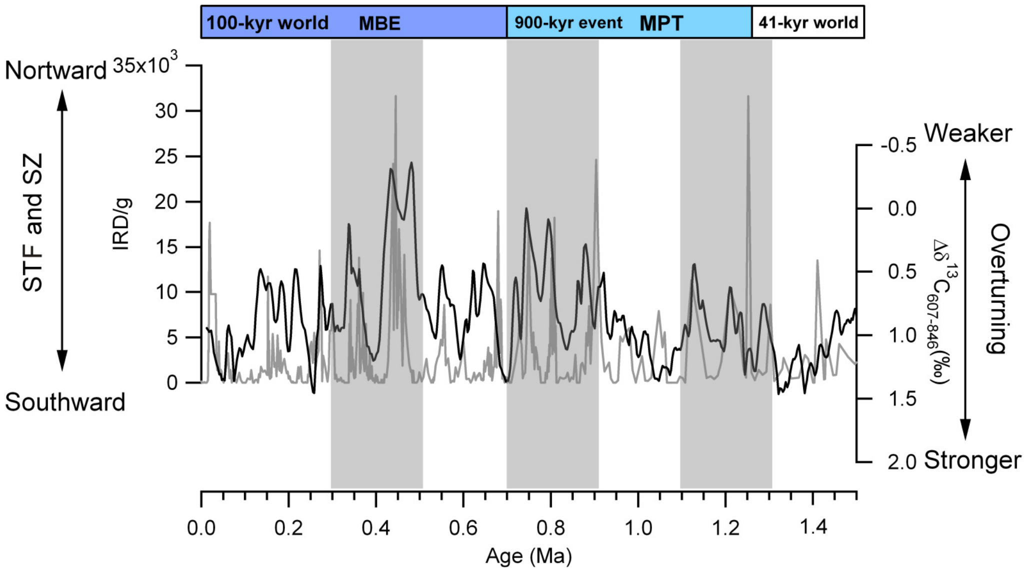

Fig. S4: $\Delta\delta^{13}C$ as an indicator of the overturning strength (12) and comparison with abundance of Ice Rafted Detritus (IRD) at ODP Site 1090 as a proxy of extreme northward migration of the STF and SZ during glacial periods (13). IRD data at ODP Site 1090 indicate extreme northward position of the STF during glacial periods every ~400 ka, at times of extreme, sustained reduction of overturning strength.

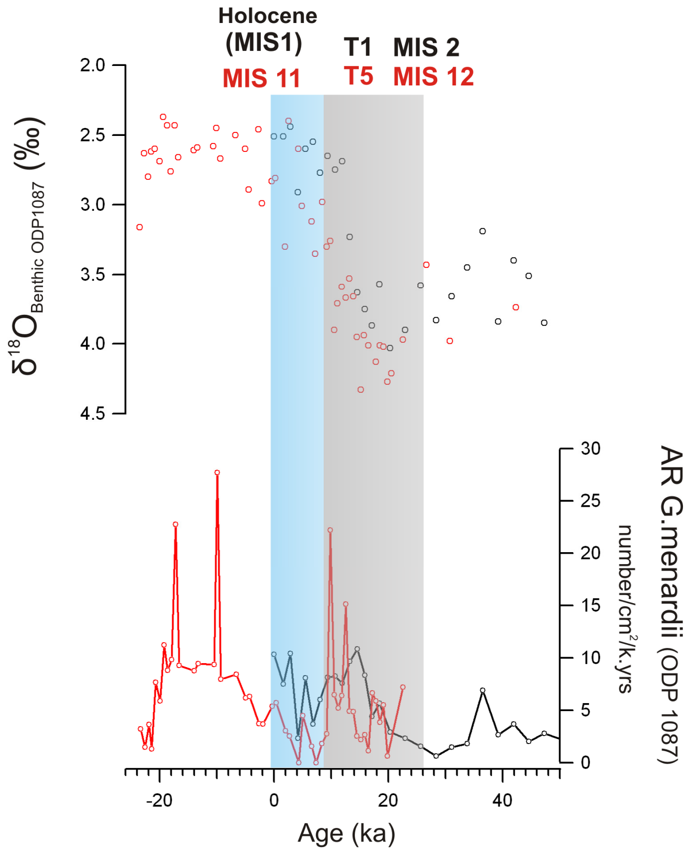

Fig. S5: Comparison between termination 1 (T1, toward the Holocene period) and termination 5 (T5, toward MIS 11 period) for the Agulhas leakage. We choose MIS 11 as a reference for comparison because 1) the low amplitude precession cycle is similar to the present day (14, 15), 2) a detailed study on MIS 11 indicates that the inter-ocean exchange of warm, salty waters into the southeast Atlantic was directly related to changes in the activity of the AMOC

(16) and 3) the Holocene period is included into a new cycle of 400 ka as it was the case for MIS 11, with moderate to high levels of G. menardii (Fig. 3). Note that the structure of events are very similar and that the period of decreased leakage during MIS 11 (blue frame) correspond to a period for which the leakage is always more important during the Holocene. Consequently, long-term natural climatic configuration of the Agulhas leakage is rather favourable for a stable and vigorous AMOC in the near future.

Supplementary information references

1. Lisiecki LE, Raymo ME (2005) A Pliocene-Pleistocene stack of 57 globally distributed benthic $\delta^{18}O$ records. *Paleoceanography*, 10.1029/2004PA001071.
2. Huybers P (2007) Glacial variability over the last two million years: an extended depth-derived agemodel, continuous obliquity pacing, and the Pleistocene progression. *Quat Sci Rev* 26:37-55.
3. Peeters FJC, *et al.* (2004) Vigorous exchange between the Indian and Atlantic oceans at the end of the past five glacial periods. *Nature* 430:661-665.
4. Paillard D, Labeyrie LD, Yiou P (1996) Macintosh program performs time-series analysis. *EOS Trans. AGU* 77, 379.
5. Caley T, *et al.* (2011) High-latitude obliquity as a dominant forcing in the Agulhas current system. *Climate of the Past* 7:1285-1296.
6. Barrows TT, Steve J (2005) Sea-surface temperatures around the Australian margin and Indian Ocean during the last glacial maximum. *Quat Sci Rev* 24:1017-1047.
7. Hayes A, Kucera M, Kallel N, Sbaffi L, Rohling EJ (2005) Glacial Mediterranean sea surface temperatures based on planktonic foraminiferal assemblages. *Quat Sci Rev* 24:999-1016.
8. Kucera M, *et al.* (2005) Reconstruction of sea-surface temperatures from assemblages of planktonic foraminifera: multi-technique approach based on geographically constrained calibration datasets and its application to glacial Atlantic and Pacific Oceans. *Quat Sci Rev* 24:951-998.
9. Kroon D, Steens T, Troelstra SR (1991) Onset of monsoonal related upwelling in the western Arabian Sea as revealed by planktonic foraminifers. *Proc. ODP Scientific Results* 117.
10. Chen MT, Farrell JW (1991) Planktonic foraminifer faunal variations in the northeastern Indian Ocean: A high-resolution record of the past 800 000 years from site 758. *Proc. ODP Scientific Results* 121.
11. Jian Z, *et al.* (2000) Foraminiferal responses to major Pleistocene paleoceanographic changes in the southern South China Sea. *Paleoceanography*, 10.1029/1999PA000431.
12. Bard E, Rickaby, EM (2009) Migration of the subtropical front as a modulator of glacial climate. *Nature* 460:380-383.
13. Becquey S, Gersonde R (2002) Past hydrographic and climatic changes in the Subantarctic Zone of the South Atlantic-The Pleistocene record from ODP Site 1090. *Palaeogeogr Palaeoclimatol Palaeoecol* 182:221-239.
14. Berger A, Loutre MF (2002) An exceptionally long interglacial ahead?, *Science* 297:1287-1288.
15. Loutre MF, Berger A (2003) Marine isotope stage 11 as an analogue for the present interglacial. *Global Planet. Change* 36:209-217.
16. Dickson AJ, *et al.* (2010) Atlantic overturning circulation and Agulhas leakage influences on southeast Atlantic upper ocean hydrography during marine isotope stage 11. *Paleoceanography* 25:PA3208.